Coupling between the Iberian basin–scale circulation and the Portugal boundary current system. A chemical study

Fiz F. Pérez*, Carmen G. Castro, X.A. Álvarez–Salgado and Aida F. Ríos

CSIC, Instituto Investigacións Mariñas, Eduardo Cabello 6, E36208 Vigo (Spain)

Abstract

The role played by the Portugal Current System in the ventilation of the different modes of Eastern North Atlantic Central Water (ENACW) is evaluated on basis of a series of cruises carried out along the western coast of the Iberian Peninsula. Results show the Portugal Current, located west of 10.3°W, conveying fresh modes of recently ventilated ENACW of subpolar origin to the south. Within 70 km from the slope, the Portugal Coastal Countercurrent transports northwards low oxygen/high nutrient ENACW of subtropical origin. Downstream ventilation of ENACW of subtropical origin occurs due to mixing and/or entrainment with offshore ventilated ENACW. We point to mesoscale eddies as the main mechanism for this downstream indirect ventilation, which reconciliate opposite views from direct current measurements and hydrographic studies.

Keywords: Circulation, watermasses, ventilation, North Atlantic, Iberian Basin

*Corresponding author. Fax: +34 986 29 27 62; email: fiz@iim.csic.es

Revised manuscript submitted to *Deep–Sea Research I*, date 16–06–00

1. Introduction

Northeast of the Azores Front there is a region of weak circulation bounded to the north and south by the North Atlantic Current (NAC) and the Azores Current respectively, and to the east and west by Europe and the Mid–Atlantic Ridge (Maillard 1986). Considering that the NAC and the Azores Current respectively bound the subpolar and subtropical gyres, then this weak circulation region is an intergyre zone (Pollard et al., 1996). The northern part of this zone (approximately north of 45ºN) is characterised by strong winter convection, being the formation area of the Eastern North Atlantic Central Water Subpolar mode (ENACWsp), with density anomalies between 27.0 and 27.2 (McCartney and Talley, 1982; Harvey, 1982; Paillet and Arhan, 1997). South of 45ºN, a wedge of saline water (S> 35.7) is associated with the northern outcrop of the anticyclonic gyre (Pollard and Pu, 1985). In this region, the large–scale circulation is weak, eastward or south–eastward. Krauss (1986) showed a similar pattern from surface current measurements (Fig. 1). He divided the intergyre region in *i*) a northern regime, where the NAC shows a broad west wind drift (line A'), and *ii)* a southern regime, where the subtropical gyre can expand (line A). The area between A and A' belongs temporarily to the northern or southern regimes. The Portugal Current (PC) receives its water from this transition zone.

The geostrophic field from historical databases shows a weak south–westward flow from the southeastern side of the NAC (Helland–Hansen and Nansen, 1926; Dietrich, 1969, Wegner, 1973; Saunders, 1982). Currentmeter data indicate that the intergyre zone is also crossed by several southeastward branches of the NAC (Krauss, 1986). Both schemes show the equatorward PC as a characteristic feature of the upper circulation in the Iberian Basin with little seasonality in the dynamic field (Maillard, 1986). Within 70–80 km from shore a prevalent poleward flow (~200 m deep) was

described in autumn and early winter, conveying ENACW of subtropical origin (S> 35.7), ENACWst (Haynes and Barton, 1990; Pingree and Le Cann, 1990; Frouin et al., 1990; Castro et al., 1997). This poleward current, coined as the Portugal Coastal Countercurrent (PCCC) by Ambar and Fiúza (1994), is induced by geostrophic adjustment of the weak eastward oceanic flow driven by large–scale meridional baroclinic pressure gradient (Frouin et al., 1990), though it responds rapidly to the applied alongshore wind–stress (Haynes and Barton, 1990). During the upwelling season (from April–May to September–October), the PCCC vanishes due to the predominance of northerly winds. However a subsurface poleward flowing Portugal Coastal Under Current (PCUC) centred at 100–200m still transports ENACWst (Álvarez–Salgado et al, 1993; Castro et al., 1994; Castro et al., 2000). Recently, Paillet and Mercier (1997) achieved to model these dynamic features applying an inverse model for the Eastern North Atlantic. Mazé et al. (1997) described similar features in the volume transport of the Iberian Basin, with a poleward flow along the Eastern boundary (<10.5ºW) and a weak southward flow in the open ocean (>10.5ºW).

Pollard and Pu (1985) estimated ventilation times from 7 to 20 years for ENACWsp in the Subtropical Front on basis of the downstream oxygen consumption, as this water mass is conveyed southward by the PC. On the other hand, according to the circulation scheme of the Portugal Current System, we should expect a downstream nutrient enrichment in ENACWst as it is transported northward by the PCCC. However, independent chemical determinations along this eastern boundary show a northward decrease (increase) of nutrient (oxygen) levels in ENACWst (Manríquez et al., 1976; Coste et al., 1986; Pérez et al., 1993).

The aim of the present manuscript is to match the above opposite dynamic and chemical features of ENACWst. We will first establish the Iberian basin–scale patterns

of ENACW ventilation with observations collected during the Bord–Est 3 cruise (Arhan et al., 1991). Then, we will propose a possible mechanism of ENACWst ventilation based on data collected during cruises MORENA I (May 1993) and GALICIA VI (December 1983). A well–defined PCCC was observed along the slope of the Iberian Peninsula during these two latter cruises and it was sampled in denser spatial detail.

2. Data set and methods

The Bord–Est 3 (BE3) cruise was carried out from 9 to 26 May 1989 on board R/V 'Le Suroit'. The cruise consisted of one meridional and three zonal transects off the Iberian basin (Fig. 2) between 36ºN and 46ºN (Arhan et al., 1991). The MORENA I cruise was performed on board R/V 'Cornide de Saavedra' from 10 to 26 May 1993 and consisted of 92 stations from 40°N to 43ºN and from the coast to 11°W along 13 transects perpendicular to the western Iberian coast (Fig. 2). In both cruises a CTD–rosette sampler was used to measure temperature, salinity and pressure and collect samples for nutrients and oxygen analyses. Nutrients were determined by colorimetric methods, using a Technicon autoanalyser. Nitrate was determined after reduction to nitrite in a Cd–Cu column (Mouriño and Fraga, 1985). The standard deviation for duplicates analyses was 0.05 $\mu mol \cdot kg^{-1}$, *i.e.*~0.5% full scale. The classical Winkler method was used to measure dissolved oxygen concentrations. A Pt combined electrode was used to determine the end point of the titration with an accuracy of 0.5 $\mu mol \cdot kg^{-1}$. These data are available at the British Oceanographic Data Centre.

The Galicia VI cruise was executed from 1 to 12 December 1983 aboard R/V 'Garcia del Cid' at the time of the strong poleward flow observed by Frouin et al., (1990) along the continental slope of the Iberian Peninsula. It covers 8 zonal sections from 40°N to 47ºN (Pérez et al., 1985). The southernmost transect of this cruise was selected for comparison with a similar section during the MORENA I cruise (Fig. 2).

Casts of 5 litre PVC Niskin bottles with attached reversing thermometer frames were used in this cruise. Salinity was determined from conductivity measurements (UNESCO, 1985) using an AUTOSAL 8400 A. Oxygen and nutrients methods were the same as previously described for the BE3 and MORENA I cruises. Potential temperature (θ) has been used throughout this manuscript.

The geopotential anomaly at 120 dbar was computed relative to 2500 dbar. Water displacements at this reference level are very slow according to Mazé et al. (1997). For slope stations, where the water depth (Z) is shallower than the reference level, we have extended the density profiles pasting the density profile (from Z down to 2500 dbar) of the closest station in deeper waters. This is equivalent to consider that the velocity between the pair of deep and slope stations in the Z–2500dbar range is zero.

The best fit between any pair of dependent (Y) and independent (X) variables was obtained by minimising

$$\sum_i \left[\left(X_i - \hat{X} \right)^{w_X} \times \left(Y_i - \hat{Y} \right)^{w_Y} \right]^2$$

Where w_X and w_Y are weights for the independent and dependent variables respectively, with w_X, $w_Y > 0$ and $w_X + w_Y = 1$. The weight factors must be a function of the estimated experimental error of the measured variables (er_X, er_Y) compared to the standard deviation (SD_X, SD_Y) of the whole set of measurements of this variable. For a given pair of variables,

$$w_X = \left(\frac{er_X}{SD_X} \right) \Big/ \left(\frac{er_X}{SD_X} + \frac{er_Y}{SD_Y} \right)$$

In order to simplify the linear regressions analyses, all possible cases were condensed to 2 categories or models: (I) $w_X = 0$, $w_Y = 1$; and (II) $w_X = w_Y = 0.5$ (Sockal and Rohlf 1995). Model I was used when $w_Y >> w_X$ as it occurs with any chemical

variable vs. temperature or salinity. Model II was used when $w_X \approx w_Y$, *i.e*. when X and Y were chemical variables. Differences between models I and II increase as the correlation coefficient (*r*) decreases. The probability level of the regression is given by the *p*–level.

3. Results and discussion

3.1. ENACW variability at the scale of the Iberian Basin (BE3 observations)

Figure 3a shows the θ/S diagram for water samples collected during the BE3 cruise in the depth range of central mode waters (100–500m). ENACW observed during this cruise follows closely the reference lines defined by Ríos et al. (1992). However, oxygen and nitrate variability is somewhat more complex. For each zonal transect (37ºN, 41ºN and 43ºN), and even for the meridional transect at 9ºW, oxygen concentrations show a linear increase with temperature. However a progressive shift with latitude is observed, presenting higher oxygen levels at higher latitudes for the same temperature (Fig. 3b). This trend parallels the decrease of oxygen saturation with increasing temperature and the southward increase of temperature for the upper layer of ENACW. Nitrate concentrations follow the opposite trend (Fig. 3c): nitrate levels decrease with increasing temperature. Likewise, there is also a marked meridional variability: for a given temperature, nitrate levels decrease northwards.

Due to the high correlation between salinity and temperature in the ENACW domain ($r > 0.97$, $p < 0.001$ for the three study cruises), the effect of ENACW modes mixing on the oxygen and nitrate variability can be adequately removed by linear regression with either salinity or temperature. Temperature is preferred because its range/precision ratio is 4–fold that of salinity. The linear regressions (model I) for oxygen and nitrate with temperature for all samples corresponding to ENACW during cruise BD3 are:

$$O_2\ (\pm 13) = 170\ (\pm 8) + 4.7\ (\pm 0.7)\cdot\theta \quad [r= 0.40,\ n= 206,\ p<0.001] \tag{1}$$

$$NO_3^-\ (\pm 1) = 42(\pm 1) - 2.7\ (\pm 0.1)\cdot\theta \quad [r= 0.86,\ n= 206,\ p<0.001] \tag{2}$$

The correlation between oxygen and nitrate anomalies (measured – calculated; Fig. 3d) is significant (r^2= 0.94) with a slope R_N (= $-\Delta O_2{:}\Delta NO_3$) equal to 6.4±0.2 (n= 206). Thus, about 94% of the oxygen and nitrate variability not fitted by mixing of ENACW modes can be explained by processes of remineralization of organic matter (ROM). However, the calculated slope is somewhat lower than the theoretical R_N value of 9.3 (Redfield et al., 1963; Anderson, 1995) and previous field determinations (Takahashi et al., 1985; Minster and Boulahdid, 1987; Fraga and Pérez 1990; Castro et al., 1998). Castro (1997) showed that the low R_N values in the Iberian basin are due to the low preformed nitrate concentrations of ENACWsp, related with the poleward intrusion of ENACWst.

3.2. ENACW ventilation on the Portugal Current System

3.2.1. Thermohaline and geostrophic fields during a PCCC event

South–westerly winds prevailed during the MORENA I cruise, with an average of 6.3 $m\cdot s^{-1}$ and a maximum of 15 $m\cdot s^{-1}$, which favoured the development of the surface PCCC. Fig. 4 shows the horizontal distributions of θ, salinity, density anomaly and geopotential anomaly at 120 dbar. The upper limit of ENACW (identified by a shallow subsurface salinity maximum) all over the study area was between 75 and 105 dbar. ENACWst with θ> 13ºC (Fig. 4a) and S> 35.75 (Fig. 4b) occupied this horizon, except in the north–west corner (stns 3 to 5; Fig. 1). The distribution of thermohaline

properties was meridional rather than zonal, in opposite to the climatology of the Eastern North Atlantic (Maillard, 1986). The northward spreading of ENACWst is traced by temperature and salinity maxima that extend from 10.2ºW at 40.5ºN to 9.8ºW at 43ºN (dotted lines in Fig. 4). In opposite direction, temperature and salinity minima stretched out from 43ºN to nearly 41ºN along 10.5ºW (dashed lines in Fig. 4). However, there was a gap at the 41.8ºN section associated to an eastward intrusion of saline and warm water during a short period (15 to 17 May) of strong south–westerly winds (15 $m \cdot s^{-1}$). Salinity and temperature minima observed at the shelf break suggest deepening in association with the convergence between the high salinity core of ENACWst on the slope and the fresher and cooler shelf waters. The density anomaly field (Fig. 4c) clearly shows the northward spreading of the lighter ENACWst between the shelf break and the ENACW located west of 10.3ºW. The 120db/2500db geopotential anomaly field (Fig. 4d) shows alternating southward and northward geostrophic currents associated with the fronts between the warm and saline ENACWst wedge and **1**) shelf waters, to the coast (east); and **2**) cold and less saline modes of ENACWst, to the open ocean (west). It should be noticed that ENACWsp occupied the north–western corner at this 120db horizon.

The selected θ–S profiles in Figure 5 also show the spatial variability of the water masses during the MORENA I cruise. It is worth noting that this θ/S relationships were shifted towards higher salinity and/or lower temperature compared with the ENACW reference line (Fiúza, 1984; Ríos et al., 1992) due to the strong saline change occurred in 1991 (Pérez et al. 1995, Pollard et al., 1996). The θ/S relationships for ENACW of stns 4 and 5 (43ºN) were rather close to the ENACW reference line and their salinity maxima were relatively fresh (S< 35.72). On the other hand, the θ–S profile of stn 91 covered the largest ENACW temperature and salinity ranges, with a

salinity maximum as high as 36.14. For the rest of stations, ENACW presented θ/S relationships between the extreme θ–S profiles of stn 5 and 91. Two specific θ–S profiles at stn 65 (41ºN, 10.32ºW) and at stn 2 (43ºN, 9.8ºW) were practically coincident in the upper 150m, although their positions were quite distant (Fig. 2). The θ/S segment for ENACW at stn 65 was only slightly fresher or warmer than that of stn 2. In fact, stations 2, 9, 22, 49, 52 and 65, located along the northward–flowing geostrophic current (see stars in Fig. 4d) show very close θ–S profiles (Fig. 5). However, the θ–S profile of stn 64 was quite different from that of stn 65, whilst it was very similar to the θ–S profile at stns 42 (41.8ºN, 9.8ºW) and 53 (not shown). It should be noticed that the line of maximum geopotential anomaly and minimum density linked stns 42, 53 and 64. Therefore, the analysis of water mass properties presented additional evidences of the northward spreading of the saline and warm ENACWst.

The hydrographic and dynamic fields during the MORENA I cruise differed from the large spatio–temporal average fields (Maillard, 1986). The observed mesoscale physical structure reflects a north–south exchange of water along two opposite paths. During the northward spreading of the warm and saline wedge of ENACWst along the slope of the Iberian margin, it mixes either with shelf waters to the east or with fresh and cold ENACW (either subpolar or subtropical) to the west.

3.2.2. Chemical fields during two contrasting PCCC events (MORENA I and Galicia VI observations)

The BE3 data have clearly shown a northward decrease (increase) of ENACW nitrate (oxygen) levels for a given temperature (Fig. 3) at the Iberian basin scale. Therefore, the intense PCCC recorded during the MORENA I cruise (Figs 4, 5) should transport northwards along the slope warm, low–oxygen and high–nutrient ENACWst,

whereas the PC should transport southwards colder, high–oxygen and low–nutrient ENACW. After the first descriptions of the PCCC along the Iberian slope in autumn and winter (Haynes and Barton, 1990; Pingree and Le Cann, 1990; Frouin et al., 1990), Krauss' (1986) circulation cartoon (Fig. 1) was modified by Ellett (1993). This author considered that, on the light of the field observations, two opposite currents should constitute the Portugal Current System but he did not go in any detail on their extension, coexistence or seasonality. Mazé et al. (1997) suggested a seasonal alternation of the PC and PCCC along the Iberian margin to explain the southward penetration of ENACWsp and the northward penetration of ENACWst. In the preceding section, we have shown how the PC and PCCC can coexist as suggested by Ambar and Fiúza (1994), leading to a quite intricate circulation pattern. In this section, we will demonstrate that mixing and/or entrainment of the contrasting water masses transported by the opposite flows produces a downstream modification of their chemical properties.

Following the same procedure than with the BE3 data, the effect of ENACW modes mixing on the oxygen and nitrate fields has been removed considering the anomalies of their respective linear regressions with temperature (model I):

$$O_2(\pm 8) = 171(\pm 7) + 4.4\ (\pm 0.5)\cdot\theta \quad [r = 0.43,\ n = 264,\ p < 0.001] \tag{3}$$

$$NO_3^-(\pm 1) = 45.8\ (\pm 0.9) - 2.98\ (\pm 0.07)\cdot\theta \quad [r = 0.93,\ n = 264,\ p < 0.001] \tag{4}$$

The differences between the regressions for BE3 and MORENA I are due to the different spatial coverage of both cruises; the latitudinal range of MORENA I was 3º, about 1/3 the extension of BE3. Nitrate and oxygen anomalies for the MORENA I data are highly correlated (r^2 = 0.76) with a slope, R_N (= $-\Delta O_2{:}\Delta NO_3$), of 6.5± 0.2 (n=

264), which is not significantly different from the R_N ratio obtained with the BE3 data. ROM explains ~76% of the nitrate and oxygen variability. This is lower than the percentage of explained variability for the BE3 cruise, due to the reduced spatial coverage of the MORENA I cruise as well.

Two zonal sections along 43ºN and 41ºN were selected to show the ventilation of ENACW (Fig. 6). A sigma–coordinated presentation was used to avoid changes due to vertical displacements of water masses. The salinity distribution along 43ºN shows a saline wedge, with S> 35.8, over the slope (Fig. 6a). Less saline ENACW was located west of 10.3ºW with a distinct θ/S relationship (Fig. 5, stn. 5). At the 27.1 isopycnal level (about 200 m), a front between ENACWst and ENACWsp is clearly defined. Oxygen (Fig. 6b) and nitrate (Fig. 6c) anomalies closely mirror each other. The front is associated with the 10 and –1 $\mu mol \cdot kg^{-1}$ oxygen and nitrate anomaly isopleths respectively, and separates ENACW with high oxygen and low nitrate levels to the west from ENACW with low oxygen and high nitrate over the slope. The lowest oxygen and highest nitrate anomalies are located on the shelf due to intense ROM processes (Álvarez–Salgado et al. 1997). Although the saline wedge that traces the poleward advection of ENACWst appears in the upper layers, the chemical fields depicted a deeper signature of the poleward current as well as the geostrophic velocity field (not shown).

The salinity distribution at 41ºN clearly shows a front between stns 64 and 65 (Fig. 6d). The saline core extended from 10.2ºW to the shelf–break with S> 35.95. In the upper layer, a salinity minimum was found at stn. 65. Below the upper layer, the saline distribution showed a nearly constant vertical gradient without any frontal structure. The slight tilting of the isohalines indicate a minor salinity increase of ENACW to the slope. The nitrate (Fig. 6e) and oxygen (Fig. 6f) anomaly distributions

also show good concordance. The lowest oxygen (highest nitrate) anomalies are again located over the shelf, as along 43ºN. The positive (negative) oxygen (nitrate) anomalies centred at stn. 65 trace the southward penetration of recirculated ENACWst. On the other hand, the northward advection of ENACWst is characterised by negative (positive) oxygen (nitrate) anomalies.

The 41°N section presents more negative (positive) oxygen (nitrate) anomalies than the 43°N section, following the large–scale pattern of increasing ventilation to the north (Pollard and Pu, 1985). The oxygen decrease and nitrate increase along the southward flowing branch of ENACW is in agreement with downstream ageing due to ROM. However, the nitrate decrease and oxygen increase in the northward flowing PCCC can not be explained by downstream ageing due to the ROM processes. Mixing and/or entrainment with the southward flowing ventilated ENACW are the main responsible mechanisms for this oxygen increase (nutrient decrease) of the ENACWst high salinity core as it flows northwards. The effect of mixing/entrainment on the chemical field is the same of direct ventilation when an isopycnal outcrops at sea surface, and we can considered it as a mechanism of indirect ventilation. Stn 2 (in the core of the PCCC at 43ºN) showed higher oxygen (lower nitrate) levels than stn 64 (in core of the PCCC at 41ºN), but lower oxygen (higher nitrate) levels than stn 65, with a θ–S profile similar to stn 2. The northward geostrophic current band between 10 and 10.2ºW seems to link stns 65 and 2 (Fig. 4d). However, the degree of ENACW ventilation is completely different. At 41ºN, stn 65 is occupied by ventilated ENACW coming from the north. At 43ºN, stn 2 clearly traces the PCCC transporting relatively aged ENACWst. A cyclonic circulation between both branches of ENACW could match this apparent contradiction. Two cyclonic eddies centred at 41.6º and 42.6ºN can be observed in Fig. 4d. Stn. 65 is located in the southern limb of

the cyclonic gyre centred at 41.6ºN. Thus, ENACW at 41°N could be recirculated northward. These eddies are probably responsible for the properties exchange between the poleward and the equatorward branches of ENACW. This mechanism could explain the continuous decreasing of salinity and nutrient levels in the recurrently observed poleward slope current off the Iberian Peninsula (Haynes and Barton, 1990; Pérez et al., 1993; Pingree, 1994; Castro et al., 1997).

Therefore, the mesoscale observations during the spring cruise MORENA I indicate that the northward decrease of salinity and nutrients in the ENACW domain at the Iberian margin are due to water exchange between ENACWst in the poleward slope current and the surrounding fresh and ventilated ENACWsp. However, the most intense PCCC events are usually observed in late autumn and winter (Frouin et al., 1990; Haynes and Barton, 1990; Pingree and LeCann, 1990). Although all these observations were not complemented with oxygen and nutrient determinations, the Frouin et al.'s (1990) cruise MEDPOR/2 (December 1983) was fortunately synoptic with the 41.8ºN line of the Galicia VI cruise (Fig. 2). A detailed description of the physical setting at the time of the cruise was made by Frouin et al. (1990), supported by satellite imagery. Here we just will describe the chemical setting of this strong autumn PCCC event, using the same procedure to calculate oxygen and nitrate anomalies than for cruises BE3 and MORENA I.

Along 41.8ºN, a clear high salinity core is quite apparent above 300m depth, extending from the slope to 10.3ºW (Fig 7a). Frouin et al. (1990) found the same signature of the PCCC, estimating a geostrophic transport of 0.5 Sv along the same zonal transect. The PCCC also provoked a convergence toward the shelf break, with the corresponding isotherms deepening (not shown) and the confinement of the less saline continental waters toward the coast, as observed during the MORENA I cruise.

The sigma–coordinated presentation of the haline field shows a clear front above the 27.0 isopycnal, between the core of saline ENACWst with S> 35.8 at stns 3 and 4 and the less saline ENACWsp at stn 6 located west of 10.3ºW (Fig 7b).

The corresponding nitrate (Fig. 7c) and oxygen (Fig. 7d) anomalies show good correlation (r= 0.70, n=42, p< 0.001) with a slope R_N of 6.4± 0.1, which is no significantly different from those calculated from BE3 and MORENA I data. The PCCC transported northwards aged ENACWst, which is ventilated by mixing with the low nitrate/high oxygen ENACWsp flowing southward, west of 10.3ºW (Frouin et al., 1990). Thus, this autumn cruise also confirms the circulation pattern on this eastern boundary, previously described with the spring cruise.

4. Conclusions

Poleward advection of ENACWst along the Iberian margin was first suggested by Fraga et al. (1982) —who found a subsurface front between the subtropical and subpolar branches of ENACW off Cape Finisterre, 43ºN (Fig. 1)— and confirmed by Pérez et al. (1993). Ríos et al. (1992) and Álvarez–Salgado et al. (1993) noticed a year–round increase of ENACWst salinity off the Ría de Vigo, 42ºN (Fig. 1), due to northward transport by the PCCC during the autumn, winter and spring, and by the PCUC during the summer. In the present work, the Portugal Current System was characterised chemically using data from cruises conducted under dominant southerly wind conditions (spring 89 and 93, autumn 83). In such conditions, the Portugal Current (PC) transports southward fresh modes of well–ventilated ENACW west of 10.3ºW (100–150 km off the Iberian margin). On the other hand, the PCCC moves as a high salinity core along the Iberian slope, transporting poorly–ventilated ENACWst. Exchange of ENACW between the PC and PCCC occurs, leading to a field of mesoscale cyclonic eddies that superimposes on the classical large–scale zonal

structure. As a result of this eddy–mediated exchange, ENACWsp is transported into the Subtropical Gyre, whereas aged ENACWst conveyed northward by the PCCC along the eastern boundary is indirectly ventilated with ENACWsp.

5. Acknowledgements

We would like to thank the master, officers, and crew members of the R/Vs ‘Cornide de Saavedra’ and ‘Le Noroit’ and the participants in the MORENA I and Bord–Est 3 cruises for their help. We are grateful to Trinidad Rellán for oxygen analysis and preparation of figures. Comments and suggestions of two anonymous reviewers have contributed to improve the manuscript. Financial support for this work came from the EU contract No. MAS2–CT93–65 and the Spanish CICYT contract No. AMB93–1415–CE.

6. References

Álvarez–Salgado, X.A., Rosón, G., Pérez, F.F., Pazos, Y., 1993. Hydrographic variability off the Rias Baixas (NW Spain) during the upwelling season. Journal of Geophysical Research 98(C8), 14447–14455.

Álvarez–Salgado, X.A., Castro, C.G., Pérez, F.F., Fraga, F., 1997. Nutrient mineralization patterns in shelf waters of the Western Iberian upwelling. Continental Shelf Research 17, 1247–1270.

Anderson, L.A., 1995. On the hydrogen and oxygen content of marine phytoplankton. Deep–Sea Research 42, 1675–1680.

Ambar, I., Fiúza, A.F.G., 1994. Some features of the Portugal Current System: a poleward slope undercurrent, an upwelling–related summer southward flow and an autumn–winter poleward coastal surface current. In: Katsaros, K.B., Fiúza, A.F.G., Ambar, I. (Eds), Proceedings of the second International Conference on Air–Sea Interaction and on Meteorology and Oceanography of the Coastal Zone. American Meteorological Society, pp. 286–287.

Arhan, M., Billant, A., Colin de Verdiere, A., Daniault, N., Prego, R., 1991. Hydrography and velocity measurements offshore from the Iberian Peninsula. Bord–Est Data Report, Volume 2. Campagnes Océanographiques Françaises, nº 15.

Castro, C.G., Pérez, F.F., Álvarez–Salgado, X.A., Rosón, G., Ríos, A.F., 1994. Hydrographic conditions associated with the relaxation of an upwelling event off the Galician Coast (NW Spain). Journal of Geophysical Research 99(C3), 5135–5147.

Castro, C.G., Álvarez–Salgado, X.A., Figueiras, F.G., Pérez, F.F., Fraga, F., 1997. Transient hydrographic and chemical conditions affecting microplankton populations in the coastal transition zone of the Iberian upwelling system (NW Spain) in September 1986. Journal of Marine Research 55, 321–352.

Castro, C.G., 1997. Caracterización química del agua subsuperficial del Atlántico Nororiental y su modificación por procesos biogeoquímicos. Ph.D. Thesis, Universidad de Santiago de Compostela, 325 pp.

Castro, C.G., Pérez, F.F., Holley, S., Ríos, A.F., 1998. Characterization and modelling of water masses in the Northeast Atlantic. Progress in Oceanography 41(3), 249–279.

Castro, C.G., Pérez, F.F., Álvarez–Salgado, X.A., Fraga, F., 2000. Coupling between the thermohaline, chemical and biological fields during two contrasting upwelling events off the NW Iberian Peninsula (Galician Coast). Continental Shelf Research 20(2), 189–210.

Coste, B., Fiúza, A.F.G., Minas, H.J., 1986. Conditions hydrologiques et chimiques associées à l`upwelling côtier du Portugal en fin d'été. Oceanologica Acta 9, 149–158.

Dietrich, G., 1969. Atlas of the Hydrography of the northern North Atlantic Ocean. International Council for the Exploration of the Sea, Copenhagen, pp 1–140.

Ellett, D.J., 1993. The north–east Atlantic: A fan–assisted storage heater?. Weather 48, 118–126.

Fiúza, A.F.G., 1984. Hidrologia e dinâmica das aguas costeiras de Portugal. Ph D. thesis, University of Lisbon, 294 pp.

Fraga, F., 1981. Upwelling off the Galician coast, Northwest Spain. In: Richards, F.A. (Ed.), Coastal Upwelling Series, Vol. 1, AGU, Washighton, D.C., pp. 176–182.

Fraga, F., Pérez, F.F., 1990. Transformaciones entre composición química del fitoplancton, composición elemental y relación de Redfield. Scientia Marina 54(1), 69–76.

Fraga, F., Mouriño, C., Manríquez, M., 1982. Las masas de agua en la costa de Galicia: junio–octubre. Resultados Expediciones Científicas 10, 51–77.

Frouin, R., Fiúza, A.F.G., Ambar, I., Boyd, T.J., 1990. Observations of a poleward surface current off the coasts of Portugal and Spain during winter. Journal of Geophysical Research 95(C1), 679–691.

Harvey, J., 1982. θ–S relationships and water masses in the eastern North Atlantic. Deep–Sea Research 29(8A): 1021–1033.

Haynes, R., Barton, E.D., 1990. A poleward flow along the Atlantic coast of the Iberian Peninsula. Journal of Geophysical Research 95(C7), 11425–11441.

Helland–Hansen, B., Nansen, F., 1926. The eastern North Atlantic. Geophysizke Publicajoner 4, 1–74.

Krauss, W., 1986. The North Atlantic Current. Journal of Geophysical Research 91(C4), 5061–5074.

Manríquez, M., Fraga, F., Massol, R., 1976. Datos hidrográficos de las costas NW de España 'Campaña Galicia I'. Resultados Expediciones Científicas B/O Cornide 5, 1–18.

Maillard, C., 1986. Altas Hydrologique de l'Atlantique Nord–Est. Institut Français de Recherche pour l'Exploitation de la Mer (IFREMER), 199 pp.

Mazé, J.P., Arhan, M., Mercier, H., 1997. Volume budget of the eastern boundary layer off the Iberian Peninsula. Deep–Sea Research I 44(9–10), 1543–1574.

McCartney, M., Talley, T., 1982. The subpolar Mode Water of the North Atlantic Ocean. Journal of Physical Oceanography 12, 1169–1188.

Minster, J.F., Boulahdid, M., 1987. Redfield ratios along isopycnal surfaces–a complementary study. Deep–Sea Research 34, 1981–2003.

Mouriño, C., Fraga, F., 1985. Determinación de nitratos en agua de mar. Investigación Pesquera 49, 81–96.

Paillet, J., Arhan, M., 1997. Shallow Pycnoclines and Mode Water Subduction in the

Eastern North Atlantic. Journal of Physical Oceanography 26, 96–114.

Paillet, J., Mercier, M., 1997. An inverse model of the eastern North Atlantic general circulation and thermocline ventilation. Deep–Sea Research I, 44, 1293–1328.

Pérez, F. F., Ríos, A.F., King, B.A., Pollard, R.T., 1995. Decadal changes of the θ–S relationship of the Eastern North Atlantic Central Water. Deep–Sea Research I 42, 1849–1864.

Pérez, F.F., Ríos, A.F., Fraga, F., Mouriño, C., 1985. Campaña GALICIA VI, datos básicos. Datos Informativos Instituto de Investigaciones Pesqueras 11, 38pp.

Pérez, F.F., Mouriño, C., Fraga, F., Ríos, A.F., 1993. Displacement of water masses and remineralization rates off the Iberian Peninsula by nutrient anomalies, Journal of Marine Research 51, 869–892.

Pingree, R.D., 1994. Winter warming in the southern Bay of Biscay and lagrangian eddy kinematics from a deep–drogued argos buoy. Journal of the Marine Biological Association of the U.K. 74, 107–128.

Pingree, R.D., Le Cann, B., 1990. Structure, strength and seasonality of the slope currents in the Bay of Biscay region. Journal of Marine Biology Association of the U.K. 70, 857–885.

Pollard, R. T., Pu, S., 1985. Structure and circulation of the upper Atlantic Ocean northeast of the Azores. Progress in Oceanography 14, 443–462.

Pollard, R. T., Griffiths, M.J., Cunningham, S.A., Read, J.F., Pérez, F.F., Ríos, A.F., 1996. Vivaldi 1991– A study of the formation, circulation and ventilation of Eastern North Atlantic Central Water. Progress in Oceanography 37, 167–192.

Redfield, A.C., Ketchum, B.H., Richards, F.A., 1963. The influence of organisms on the composition of sea–water. In The Sea, Volume 2, J. Wiley and Sons, New York, pp. 26–77.

Reid, J.L., Mantyla, A.W., 1976. The effect of the geostrophic flow upon coastal elevations in the northern North Pacific. Journal of Geophysical Research 81(18), 3100–3100.

Ríos, A. F., Pérez, F.F., Fraga, F., 1992. Water masses in the upper and middle North Atlantic Ocean east of the Azores. Deep–Sea Research 39, 645–658.

Saunders, P. M., 1982. Circulation in the eastern North Atlantic. Journal of Marine Research 40, 641–657.

Sockal, R.R., Rolhf, F.J., 1995. Biometry. Freeman and Company (eds), New York, 887pp.

Takahashi, T., Broecker, W.S., Langer, S., 1985. Redfield ratio based on chemical data from isopycnal surfaces. Journal of Geophysical Research 90(C4), 6907–6924.

UNESCO, 1985. The international system of units (SI) in oceanography. UNESCO Technical Papers on Marine Science 45, 1–124.

Wegner, G., 1973. Geostrophische Oberflachenstromung im nordichen Nordatlantische Ozean im Internationalen Geophysikalischen Jahr 1957/8. Berich der Deutschen wissenschaftlichen kommission für Meeresforschung 22,411–426.

Figures legends

Fig. 1. Circulation in the upper layers of the northern North Atlantic as derived from drift experiments (adapted from Krauss, 1986). **LC**, Labrador Current; **NAC**, North Atlantic Current; **GS**, Gulf Stream; and **PC**, Portugal Current. Meridionally–ruled area, flow associated with the NAC toward the north. Zonally–ruled area, flow associated to the northern limb of the Subtropical Front. Numbers are transports in Sverdrups (1 Sv = 10^6 m^3 s^{-1}).

Fig. 2. Sampling grids during cruises Bord–Est 3 (9 to 26 May 1989), MORENA I (12 to 26 May 1993) and Galicia VI (1 to 12 December of 1983). The 1000m–depth isobath is shown. Black lines correspond to the zonal transects presented in Figs. 6, 7.

Fig. 3. The ENACW domain during cruise Bord–Est 3 (9 to 26 May 1989). (**a**) θ–S diagram of ENACW samples showing the θ/S reference line of subtropical and subpolar ENACW modes by Ríos et al. (1992). (**b**) Oxygen *vs*. potential temperature plot, showing the latitudinal and vertical variability; the oxygen saturation line is also included. (**c**) Nitrate *vs.* potential temperature plot showing the latitudinal and vertical variability. (**d**) Oxygen (ΔO_2) *vs.* nitrate (ΔNO_3^-) anomalies. Salinity in psu, temperature in °C, and oxygen and nitrate in $\mu mol \cdot kg^{-1}$.

Fig. 4. Horizontal distributions at 120m depth of (**a**) potential temperature; (**b**) salinity; (**c**) density anomaly; and (**d**) geopotential anomaly relative to 700 db during the MORENA I cruise (12 to 26 May 1993). Salinity in psu, temperature in °C, density anomaly in kg m^{-3} and geopotential anomaly in $m^2 \cdot s^{-2}$. For temperature, salinity and geopotential anomaly, dotted and dashed lined denoted maxima and minima respectively. For density anomaly is the opposite.

Fig. 5. θ/S profiles of some selected stations (see Fig. 1 for locations) during the MORENA I cruise (12 to 26 May 1993). The θ/S reference line of ENACW by Ríos et al. (1992) and the 27.1 isopycnal are also shown. The enclosed graph shows the θ/S profiles of station 2, 9, 22, 49, 52 and 65, which are labelled with a star in Fig 4.

Fig. 6. Vertical distributions of salinity *vs.* depth (**a, e);** salinity (**b, f**), oxygen anomaly (**c, g**) and nitrate anomaly (**d, h**) *vs.* density anomaly along the zonal section at 43ºN; and 41ºN (see Fig. 1 for locations) during the MORENA I cruise (12 to 26 May 1993). The shadow areas coarsely represent the PCCC domain. Salinity in psu, oxygen and nitrate anomalies in $\mu mol \cdot kg^{-1}$. Shaded areas represent waters with high nutrient and low oxygen. The isotherm 13ºC and the isopycnals 26.95 (in **a**) and 26.9 (in **e**) were shown by dotted and dashed line respectively.

Fig. 7. Vertical distributions of salinity *vs.* depth (**a**); salinity (**b**), oxygen anomaly (**c**) and nitrate anomaly (**d**) *vs.* density anomaly along the 41.8ºN zonal transect (see Fig. 1 for location) during the Galicia VI cruise (1 to 12 December 1983). The shadow areas coarsely represent the PCCC domain. Shaded areas represent waters with high nutrient and low oxygen. The isopycnal 26.8 and isotherm 13ºC were shown in **(a)** by dashed and dotted line respectively.

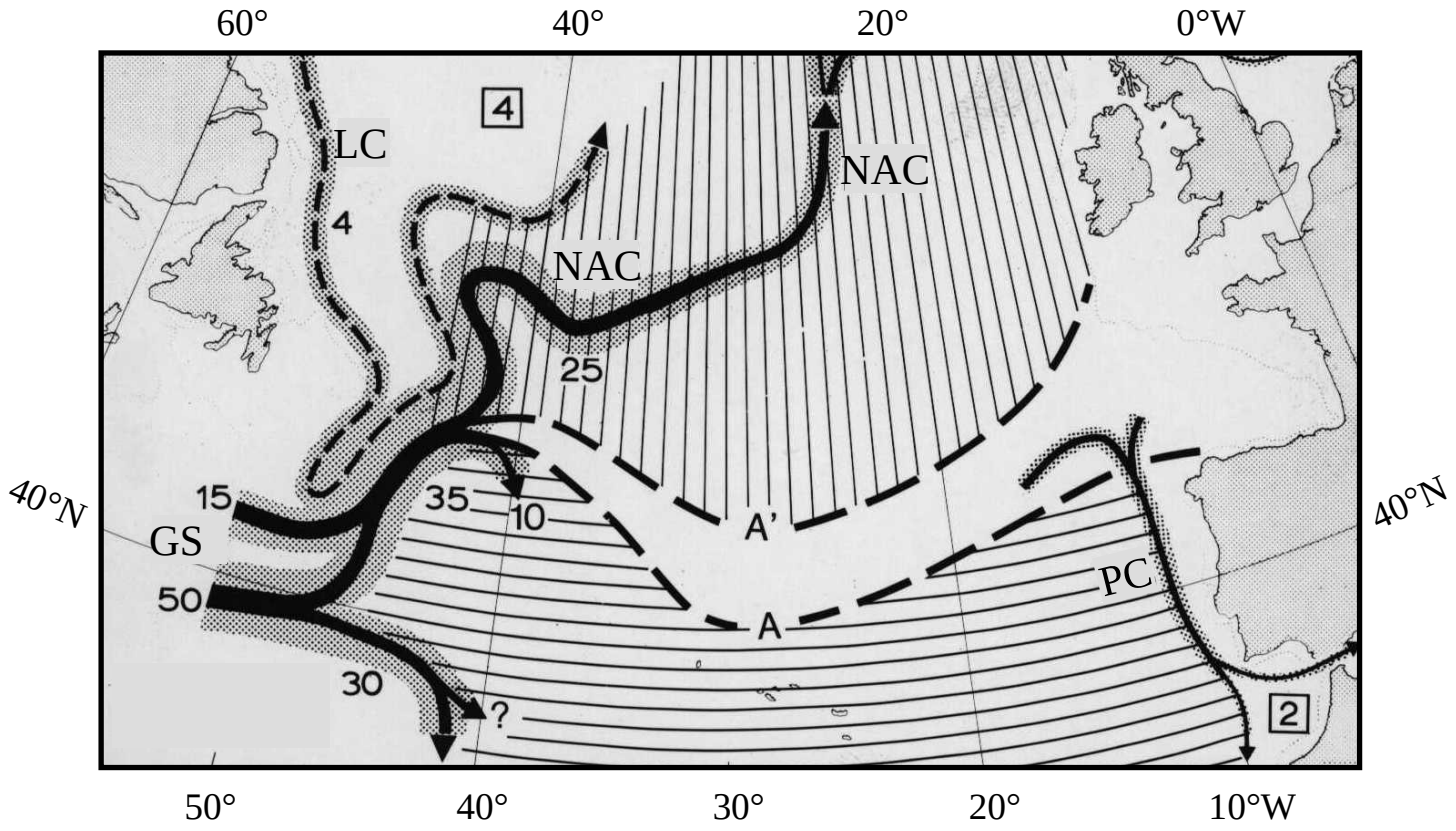

Figure 1 ‘ENACW ventilation in the Portugal Current System`’ by Pérez et al.

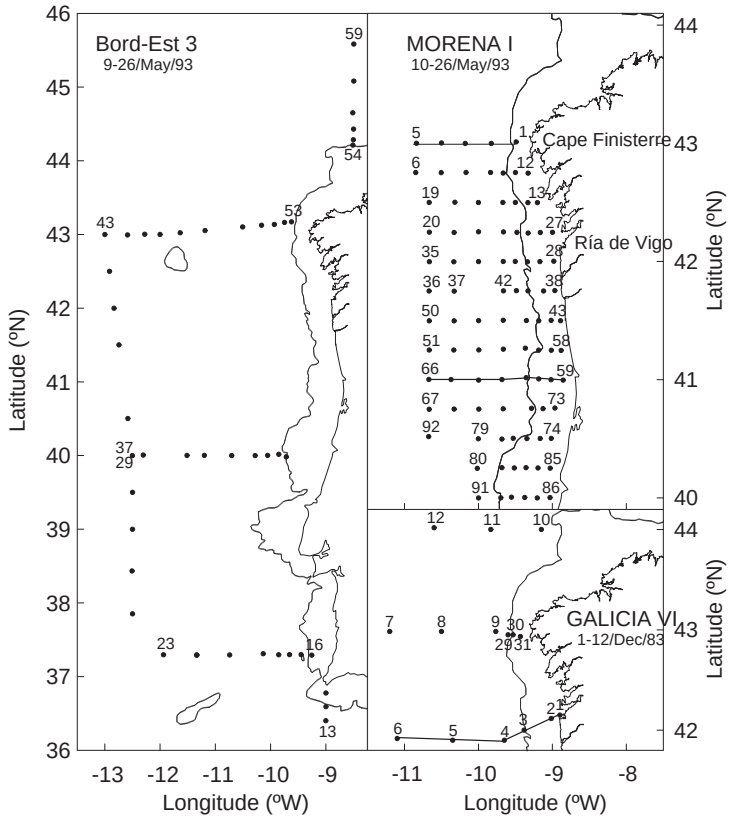

Figure 2 'ENACW ventilation in the Portugal Current System' by Pérez et al.

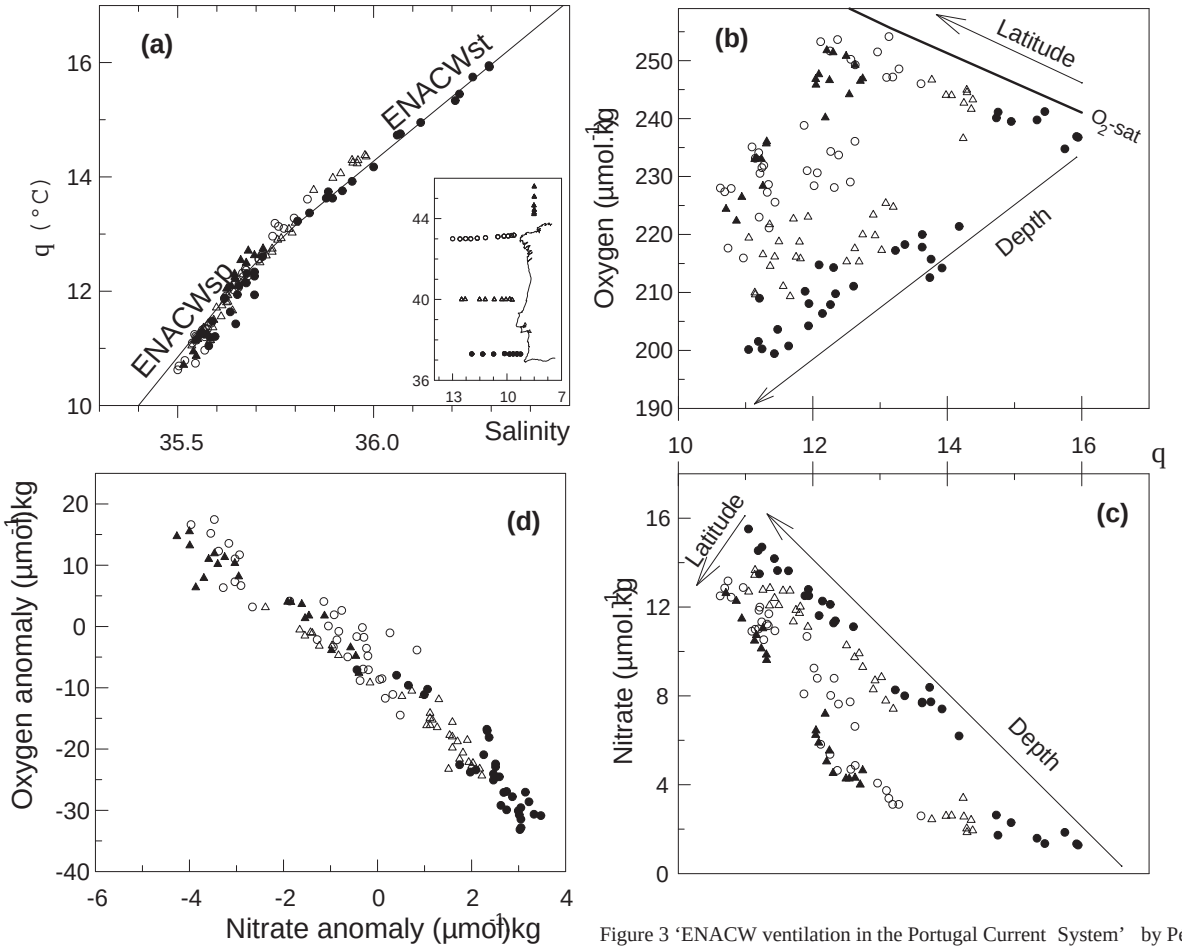

Figure 3 'ENACW ventilation in the Portugal Current System' by Pérez et al.

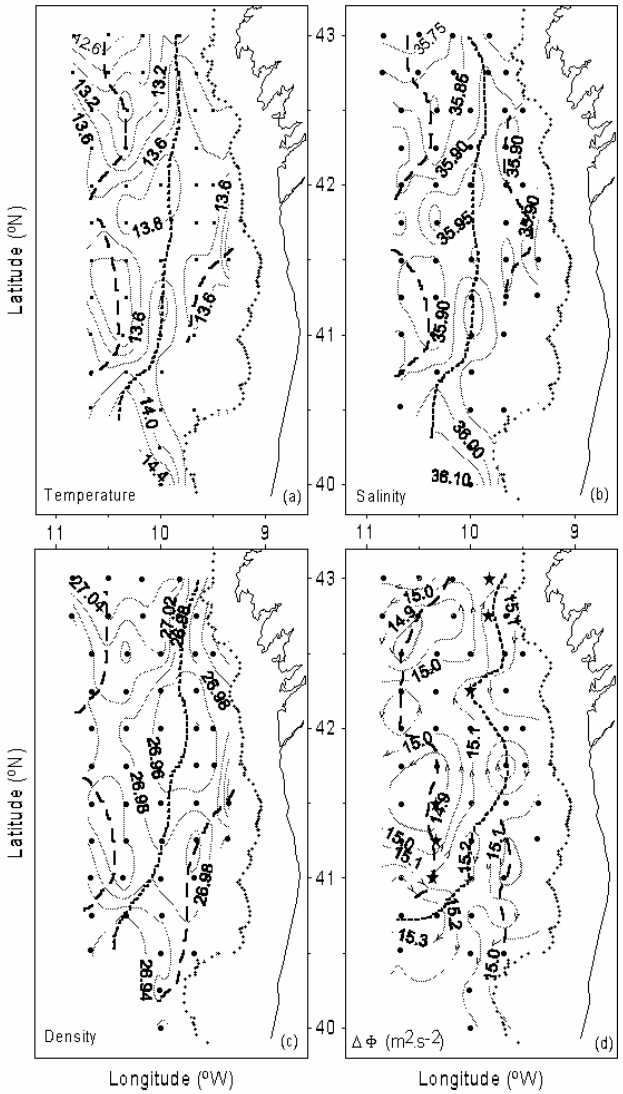

Fig 4 'ENACW ventilation in the Portugal Current System' by Pérez et al.

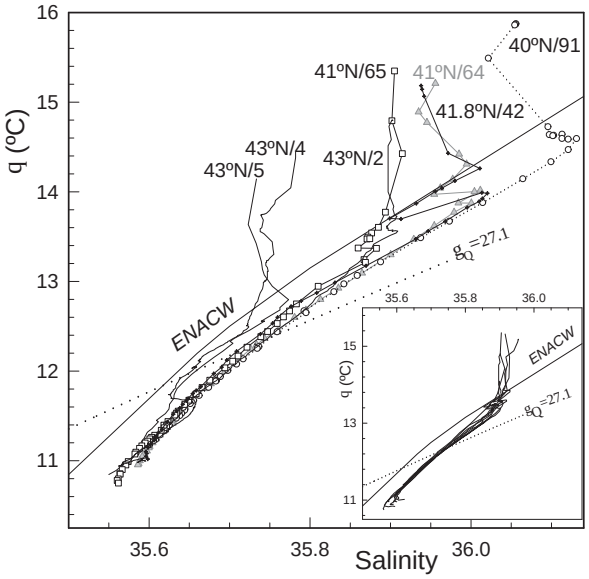

Figure 5 'ENACW ventilation in the Portugal Current System' by Pérez et al.

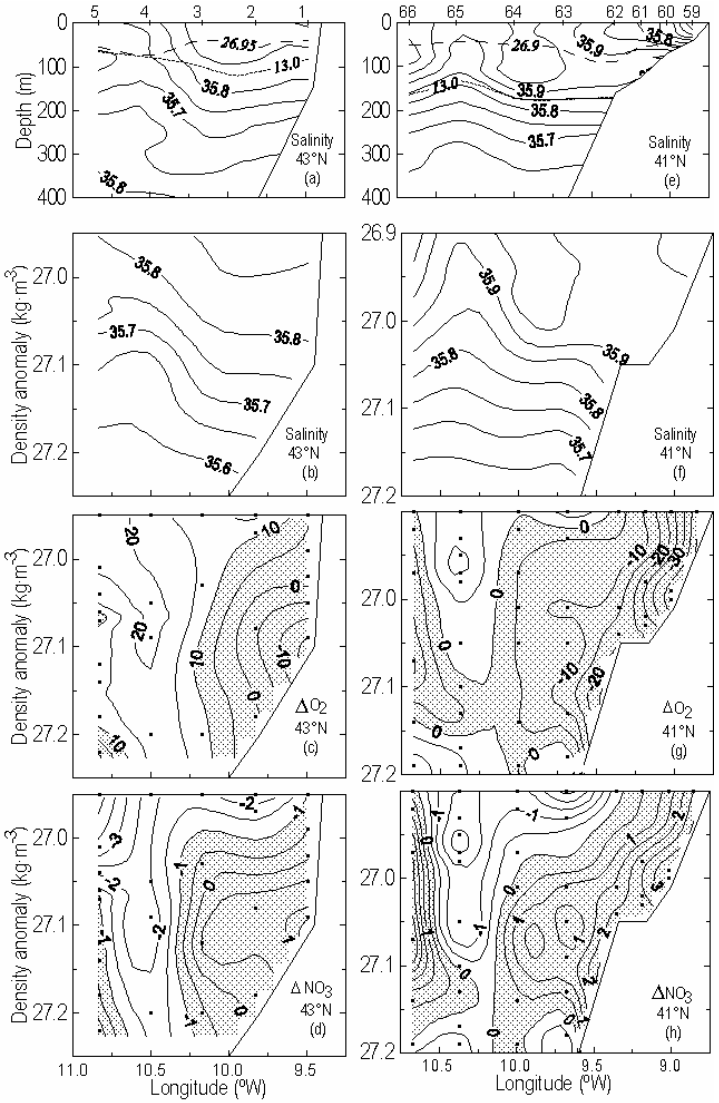

Fig. 6 'ENACW ventilation in the Portugal Current System' by Pérez et al.

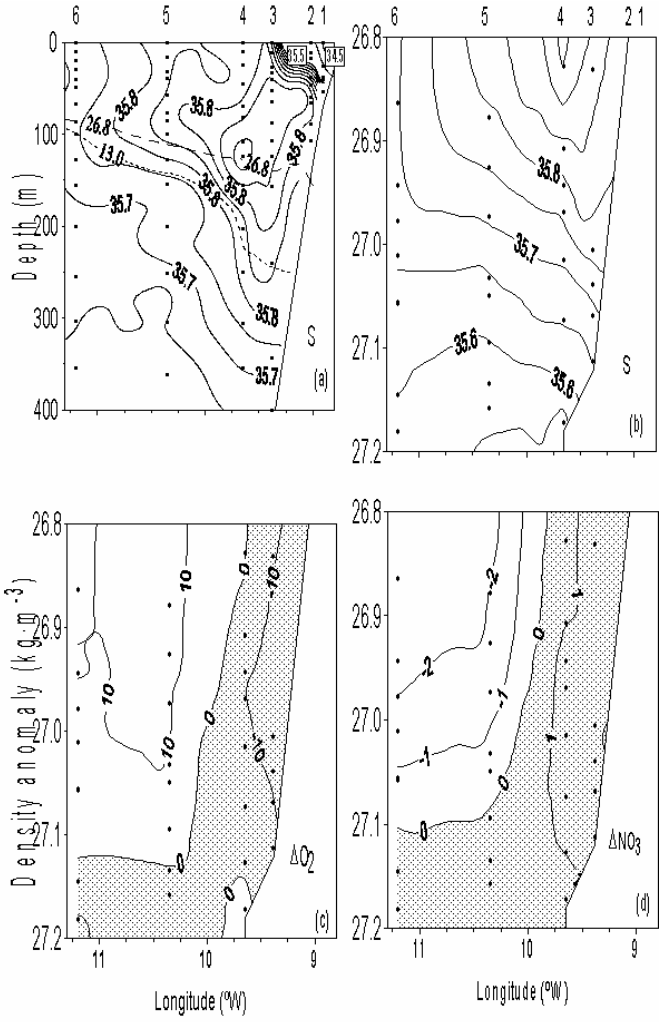

Fig 7 'ENACW ventilation in the Portugal Current System' by Pérez et al.